Journal of Applied Sciences

ISSN 1812-5654

science alert

ANSInet
an open access publisher
http://ansinet.com

Journal of Applied Sciences 14 (13): 1450-1454, 2014
ISSN 1812-5654 / DOI: 10.3923/jas.2014.1450.1454

Sawdust-derived Biochar: Characterization and CO_2 Adsorption/desorption Study

Wan Azlina Wan Ab Karim Ghani
Department of Chemical and Environmental Engineering, Faculty of Engineering,
Universiti Putra Malaysia, 43400 UPM Serdang, Selangor, Malaysia

Abstract: Sawdust-derived Biochars (SDB) was prepared in a stainless steel fixed bed pyrolyser of 43 mm height and 60 mm internal diameter at four different operating temperatures ranging from 450 to 850°C. SDB physico-chemical characterization such as surface area, functional groups and surface morphology were analyzed by N_2 physisorption, Fourier Transform Infrared Spectroscopy (FT-IR) and Scanning Electron Microscopy (SEM), respectively. SDBs to have a surface area between 10 to 200 m^2g^{-1} and FTIR revealed an aromatic functional group about 866 cm^{-1} in most biochar samples. The experimental data shows that the biochars can absorb around 5% water by mass (hydrophilic) at lower temperatures (<550°C) and FTIR results indicated that lignin is not converted into a hydrophobic polycyclic aromatic hydrocarbon (PAH) matrix. While, at higher temperature (>650°C), biochars is thermally stable and became hydrophobic due to the presence of aromatic compounds. The SDB is used for the adsorption of carbon dioxide (CO_2) and its can be apply for the removal of CO_2 from environment.

Key words: Sawdust-derived Biochar, aromatic compounds, carbon dioxide adsorption pyrolysis, fixed bed reactor

INTRODUCTION

Climate change is now a major problem worldwide due to unprecedented high levels of greenhouse gases (GHGs) in the atmosphere. Since 2000, anthropogenic carbon dioxide (CO_2) emissions have risen by more than 3% annually (IPCC, 2007), putting Earth's ecosystems on a trajectory towards rapid climate change that is both dangerous and irreversible. It was estimated that annual net emissions of carbon dioxide (CO_2), methane and nitrous oxide could be reduced by a maximum of 1.8 Pg CO_2-C equivalent (CO_2-C e) per year (12% of current anthropogenic CO_2-C e emissions; 1 Pg = 1 Gt) and total net emissions over the course of a century by 130 Pg CO_2-C e, without endangering food security, habitat or soil conservation (Lehmann *et al*., 2006). To meet this challenge, a timely and ambitious strategy is needed. Therefore, production of biochar the carbon (C)-rich solid formed by pyrolysis of biomass has been suggested as one possible means of abating climate change by sequestering carbon.

Biochar is a carbonaceous material contains 65 to 90% carbon, with the balance being volatile matter and mineral ash (Sohi *et al*., 2009). The thermal degradation of lignocellulosic materials is profoundly influenced by their chemical composition (cellulose, hemicellulose and lignin) (Lange, 2007). The feedstocks which are favoured for biochar are those that have high carbon content. These include wood and biomass from energy crops, including short rotation woody plants (e.g., *Willow*) and high productivity grasses (e.g., *Mischanthus*) and a range of herbaceous plants. They may also include abundant, available and low-cost agricultural by-products, including crop residues (including straw, nut shells and rice husks and rice hulls) (Zhang *et al*., 2004), switch grass, organic wastes including distillers grain, bagasse from sugarcane industry and olive waste (Sensoz *et al*., 2006), chicken litter dairy manure (Das *et al*., 2008) and sewage sludge and paper sludge (Shinogi *et al*., 2002). Other important criteria is the proportion of hemi-cellulose, cellulose and lignin content of the feedstock which will determined the ratios of volatile carbon (bio-oil and fuel gas) and stabilized carbon (biochar) in pyrolysis products. The selected biomass feedstocks available for biochar productions are shown in Table 1.

Although a positive effect of biochar amendments on crop yields was already apparent, to date little is known about the effects of biochar addition on carbon sequestration and consequently on the soil carbon balance. Thus, detailed investigations evaluating the

Table 1: Selected biomass feedstock available for biochar production

	Rice husk	Coconut shell	Olive bagasse	Pine barks	Sun- flower	Saw-dust	Rape
Moisture	N.A	N.A	6.8	3.0	8.1	N.A	8.8
Volatile matter	66.0	30.62	67.2	72.0	74.5	51.39	78.7
Ash[a]	20.61	26.41	4.4	1.3	17.2	14.29	14.0
Fixed carbon[a,c]	18.71	42.98	21.6	26.67	8.3	22.67	7.3
Carbon[b]	48.73	45.24	53.4	50.18	43.6	53.4	44.7
Nitrogen[b]	0.05	5.04	1.7	0.45	1.0	6.7	0.8
Hydrogen[b]	5.91	1.46	7.5	5.41	5.8	3.1	5.8
Oxygen[b,c]	44.64	48.2	37.4	43.96	49.3	36.8	48.1
L.H.V(MJ Kg^{-1})	13.5	160.7	20.0	18.61	20.5	18.0	15.3

[a]Results expressed as a percentage of dry matter. [b]Results expressed as a percentage of dry matter free of ashes. [c]Calculated by difference; N.A: Not available

thermal behaviour and structural characteristics of biochar are required before this material can be applied on the large scale is aimed in this study. The present study then to perform the characterizations of biochar properties and CO_2 adsorption/desorption of biochar produced from the pyrolysis of Malaysian sawdust in a bench-scale furnace system. This combination of methods allows us to provide new insight into the physicochemical properties of biochar as a function of temperature.

MATERIALS AND METHODS

Raw material and sample preparation: Sawdust from rubber wood (*Hevea brasilensis*) is used in this study, obtained from a local (Selangor, Malaysia) furniture manufacture. Sawdust samples were dried in crucibles in an oven at 110°C for 24 h. The samples were then ground and sieved to 2 to 3 mm particle sizes. The main characteristics of the raw sawdust are presented in Table 2.

Biochar production and characterization: The dried sawdust with particle size of 2 to 3 mm was placed in a cylindrical stainless steel fixed bed reactor of 0.43 m height and 60 mm internal diameter. The feed was heated externally by an electric heater of 3 kW capacity. The reactor temperature was regulated using a temperature controller and measured by a thermocouple in the bed. The temperature range of observation was 450 to 850°C at an interval of 100°C, with the residence time fixed at 60 min. The vapors and gases that were evolved during the process were passed through a water-cooled condenser attached to a liquid receiver, which was in turn connected to a rotary vacuum pump. The char samples were collected and sent for further analysis. The nitrogen adsorption-desorption isotherms were measured at 77 K (liquid nitrogen) on a Beckmen Coulter SA 3100 instrument. The Brunauer-Emmert-Teller (BET) surface area and total pore volume were calculated from the resultant isotherms. Fourier T ransform Infrared (FTIR)

Table 2: Main characteristics of the raw sawdust based on ASTM method D 5373

Parameter	Sawdust
Proximate analysis (wt.% dry basis)	
Volatile matter	51.39
Fixed carbon	14.29
Ash	22.67
Ultimate analysis (wt.% dry basis)	
Carbon	53.4
Hydrogen	6.7
Nitrogen	3.1
Sulfur	0
Oxygen (by difference)	36.8
Higher heating value HHV (MJ kg^{-1})	18.3

spectra of samples were recorded at room temperature on a FTIR brand equipped with an attenuated total reflection (ATR) cell. The morphologies of the samples were studied by Scanning Electron Microscope (SEM) after gold coating using a HITACHI S 3400 N instrument operating at 30 keV and equipped with EDX detector.

Gravimetric adsorption and desorption study of CO_2: The adsorption and desorption of CO_2 was studied on five biochar sample which were produced at different temperatures. Volumetric adsorption and desorption isotherms at 25°C of pure CO_2, were measured up to an equilibrium pressure of about 300 psi (~2×106 pa) utilizing a volumetric adsorption apparatus, Gravimetric Sorption Analyser (GHP-FS, with a Cahn D-200 balance, VTI Scientific Instruments, Florida) Approximately 50 mg of sorbent materials were placed in the sample chamber, which was evaluated to ~5×10-5 Torr. The amount of CO_2 adsorbed was calculated by utilizing the pressure measurements before and after the exposure of the sample chamber to CO_2. Desorption studies were conducted by gradually decreasing the pressure from 1000 psi after the adsorption cycle. After each cycle the sorbent was evacuated overnight. The adsorption isotherms were analysed by applying the Dubbin-Astakhov equation:

$$W = Woexp \{-(A/\alpha Eo)n\} \quad (1)$$

Where:

W = Volume filled at temperature T and relative pressure p/p_o

Wo = Total volume of the micro pore
A = $Rtlnp/p_o$

n, Eo and α are specific parameter of the system under investigation.

RESULTS AND DISCUSSION

SEM and BET studies of biochar: The morphologies of the biochar samples produced at different pyrolysis temperatures were done by the SEM analysis (Fig. 1). These images, indicating that the presence of aligned honeycombed-like groups of pores on the order of 10im in diameter on the surface of biochars, most likely the carbonaceous skeleton from the biological capillary structure of the raw material. In comparison to activated rubber wood, it has smooth surface areas with long ridges, resembling a series of parallel lines. Based on the surface of SEM images, the pores is cross-linked and categorized as hard woody materials (Kumar *et al*., 2006). The capillary structure is found at pyrolysis temperatures greater than 550°C shows that the structure is different as compared to the biochar formed at the lowest pyrolysis temperature (450°C). It can be explained by the fact that further temperature treatment in the range of 450 to 850°C caused micropores at hexagonal planes. This is attributed to the phenomenon where micropores become filled with tars (condensed volatiles) and other decomposition products, partially blocking porosity (Bourke *et al*., 2007). The phenomenon is verified by BET analyses which are indicated that surface area is independent of pyrolysis temperatures. The total surface area was found to be less than 10 m^2g^{-1} for the lowest pyrolysis temperature at 450°C and higher and similar surface area (about 200 m^2g^{-1}) was found at 550- 850°C. Generally, the surface area of biochar increases with increasing temperatures at which deformation occurs (Brown *et al*., 2006). However, contrasting results were observed in this study where the surface area enlargement did not occur until a pyrolysis temperature it reached at 850°C. This may be an indication that the rate of pore formation exceeded that of pore destruction, due to pore enlargement and collapse at the earlier stage and vice versa at the later stage of pyrolysis as stated previously (Yu *et al*., 2005).

Chemical characterization of biochar: FTIR spectra for the initial sawdust material and for the biochar specimen produced at 850°C are shown in Fig. 2. The sawdust

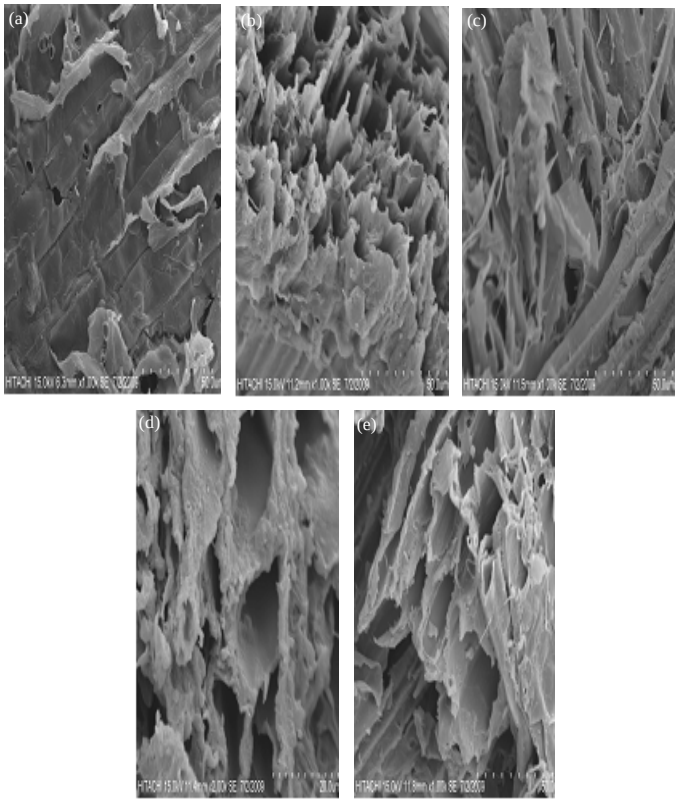

Fig. 1(a-e): SEM images of sawdust biochar samples at (a) 450°C, (b) 550°C, (c) 650°C, (d) 750°C and (e) 850°C

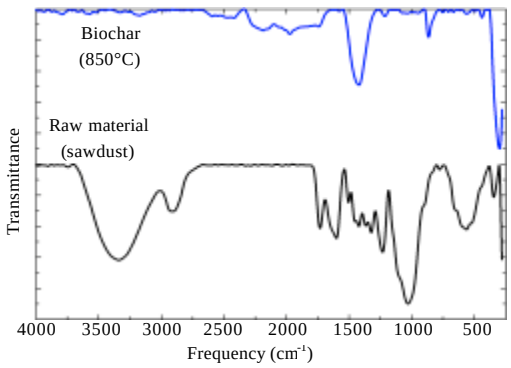

Fig. 2: FTIR spectra of sawdust raw material and 850°C biochar

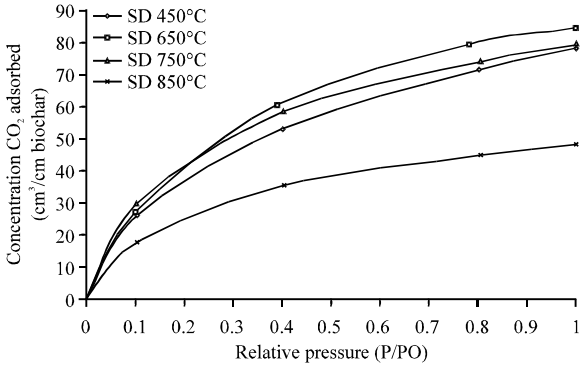

Fig. 3: Absorption and desorption isotherms of CO_2 at different production temperature of SDB

spectrum is found to be characteristic of a generic oxygenated hydrocarbon, as this sample is dominated by cellulosic biomass. The major bands have largely disappeared in the biochar sample produced at 850°C, replaced by a small number of well-defined peaks. As such, we can characterize the pyrolysis process by analysing the disappearance of bands in the raw material and the appearance of bands in the biochar samples. The original sawdust sample demonstrates a broad band between 3000-3600 cm^{-1} (peak at 3339 cm^{-1}), with a smaller band from 2700 to 3000 cm^{-1} (peak at 2907 cm^{-1}). The band centered at 3339 cm^{-1} is attributed to the presence of-OH functional groups, while the band at around 2907 cm^{-1} is likely due to alkyl C-H stretches. There is an intense band occurring at 1030 cm^{-1} which is characteristic of a C-C-O (or maybe C-O-C) asymmetric stretch. A smaller band at around 500-700 cm^{-1}, peaks at 562 cm^{-1}, could be due to -OH out of plane bending modes. There are also a number of bands between 1600 and 1800 cm^{-1}, which can be attributed to -OH in-plane bending modes, the presence of water and carbonyl (C = O) and other common alkane and oxygenated hydrocarbon functional groups. Taken together, the sawdust FTIR spectrum indicates that this material is dominated by functional groups present in oxygenated hydrocarbons, reflecting the carbohydrate structure of cellulose and hemicellulose.

Gravimetric adsorption and desorption study of CO_2: The CO_2 adsorption/desorption profiles of the produced SDBs at various temperatures are shown in Fig. 3. The adsorbed volume is plotted against the absolute relative pressure of the gas. For most of the biochar samples studied, desorption curves are overlapped with the adsorption isotherm at higher relative pressure. On the lower relative pressure, the desorption isotherm was higher than that of the adsorption isotherm which indicated that the CO_2 is not fully adsorbed during the desorption study. The hysteresis observed with biochar indicates that it is not possible to recover the adsorbed CO_2 by lowering pressure. The gravimetric studies with CO_2 suggest for biochar samples the presence of three groups of microspores, depending on their accessibility through constrictions. The first group adsorbs CO_2 molecule immediately and also desorbs quickly, which suggest that the constrictions much larger than diameter of CO_2. The second type adsorbs CO_2 very slowly and desorption require heating and, in the third case, the adsorbate is not released at all.

Furthermore, the rates of adsorption of CO_2 on biochar samples generally increases with increase in temperature from 450-650°C but decreases as the production temperature increases 750-850°C. For example CO_2 uptake at 0.5 relative pressures for biochar at 650°C was higher than the biochar at 450°C by 10% but at higher production temperature (>650°C) the CO_2 uptake for biochar was lower. This phenomenon indicates that pores at lower temperature are not fully developed but filled by disorganised carbon (tar deposition). However for higher temperature the pore sintering becomes predominant during the heat treatment at higher temperature which leads to materials with an accessible porous structure. Therefore, the relative amount of micropores can be reasonably expected to change with temperature of carbonization or treatment.

Figure 4 shows the changes in weight of CO_2 adsorbed during the adsorption and desorption process on studied biochar samples. When CO_2 is admitted in almost all biochar sample adsorbs CO_2 immediately and saturation within 50-70 min. In contrast sample biochar 650°C adsorbs a certain amount of CO_2 quickly during the first 50 min. After this rapid adsorption of 2% total amount, it takes more than 200 min to reach the

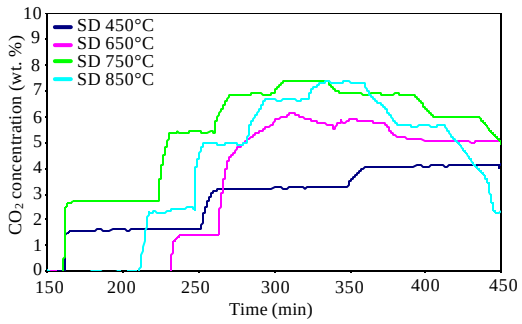

Fig. 4: Absorption and desorption profile of the biochar samples product different temperature

equilibrium. The samples exhibit a CO_2 adsorption capacity of 6.6 of CO_2 g^{-1} of biochar 450°C and up to 18 mg g^{-1} for biochar 650°C. However, with increase temperature the CO_2 uptake on biochar decreases 4.8% and 4.1% for biochar 750 and 850°C, respectively. The results reported here also shows an inverse trend with its surface area but these biochar can be used to adsorb the CO_2 from environment.

CONCLUSION

Rubber-wood Sawdust Derived Biochars (SDB) were found as softwood structures with the highest surface area of 200 m^2g^{-1} for biochar produced at 850°C. Pyrolysis temperature is found greatly influenced by both thermal and chemical properties of Rubber-wood SDB and exhibits a correspondingly large range in composition and chemistry over the studied pyrolysis temperatures. These large variations of their properties will be more effective than others in certain applications. SDB also represents a potential alternative to capture CO_2 from environment to the existing method using specialized activated carbon and molecular sieves, which tend to very expensive therefore, hinder the CO_2 sorption process due to economic constraints.

REFERENCES

Bourke, J., M. Manley-Harris, C. Fushimi, K. Dowaki, T. Nunoura and M.J. Jr. Antal, 2007. Do all carbonized charcoals have the same chemical structure A model of the chemical Struc-ture of carbonized charcoal. Ind. Eng. Chem. Res., 46: 5954-5967.

Brown, R.A., A.K. Krecher, T.H. Nguyen, D.C. Nagle and W.P. Ball, 2006. Production and characterization of synthetic wood chars for use as surrogates for natural sorbents. Org. Geochem., 37: 321-333.

Das, K.C., M. Garcia-Perez, B. Bibens and N. Melear, 2008. Slow pyrolysis of poultry litter and pine woody biomass: Impact of chars and bio-oils on microbial growth. J. Environ. Sci. Health A, 43: 714-724.

IPCC, 2007. The physical science basis: Summary for policymakers. Contribution of Working Group I to the Fourth Assessment Report of the Intergovernmental Panel on Climate Change.

Lange, J.P., 2007. Lignocellulosic conversion: An introduction to chemistry, process and economics. Biofuels, Biprod. Biorefin., 1: 39-48.

Lehmann, J., J. Gaunt and M. Rondon, 2006. Bio-char sequestration in terrestrial eco Systems: A review. Mitigation Adaptation Strategies Global Change, 11: 403-427.

Sensoz, S., I. Demirala, G.H. Ferdi, O. Bagasse and L.Oleaeuropea, 2006. Olive bagasse (*Olea europea* L.) pyrolysis. Bioresour. Technol., 97: 429-436.

Shinogi, Y., H. Yoshida, T. Koizumi, M. Yamaoka nad T. Saito, 2002. Basic characteristics of low-temperature carbon products from waste sludge. Adv. Environ. Res., 7: 661-665.

Sohi, S., E. Lopez-Capel, E. Krull and R. Bol, 2009. Biochar, climate change and soil: A review to guide future research. CSIRO Land and Water Science Report

Yu, C., Y. Tang, M. Fang, Z. Luo and K. Cen, 2005. Experimental study on alkali emission during rice straw pyrolysis. J. Eng. Sci., 39: 1435-1444.

Zhang, T., W.P. Walawender, T. Fan, M. Fan, D. Daugaard and R.C. Brown, 2004. Preparation of activated carbon from forest and agricultural residues through CO_2 activation. Chem. Eng. J., 105: 53-59.